

A numerical investigation into the correction algorithms for SPH method in modeling violent free surface flows

M. Ozbulut^a, M. Yildiz^{b,*}, O. Goren^a

^a Faculty of Naval Architecture and Ocean Engineering, Istanbul Technical University, Istanbul, Turkey

^b Faculty of Engineering and Natural Sciences, Sabanci University, Istanbul, Turkey

ARTICLE INFO

Article history:

Received 7 January 2013

Received in revised form

10 November 2013

Accepted 27 November 2013

Available online 11 December 2013

Keywords:

Violent free surface flows

SPH

Correction algorithms

ABSTRACT

A quantitative comparison of the usual and recent numerical treatments which are applied to the Smoothed Particle Hydrodynamics (SPH) method are presented together with a new free-surface treatment. A series of numerical treatments are studied to refine the numerical procedures of the SPH method particularly for violent flows with a free surface. Two dimensional dam-break and sway-sloshing problems in a tank are modeled by solving Euler's equation of motion utilizing weakly compressible SPH method (WCSPH). Initially, the dam-break benchmark problem is studied by adopting only conventional basic equations of SPH without any numerical remedy and then by considering numerical treatments of interest one after another. In the WCSPH method, the precise calculation of the densities of the particles is vital for the solution, accordingly a density correction algorithm is presented as a basic numerical treatment. Subsequently, Monaghan's (1994) [1] XSPH velocity variant algorithm, artificial particle displacement (APD) algorithm (Shalduo et al., 2011) [2], and a hybrid combination of velocity updated XSPH (VXSPH) and APD algorithms are implemented separately, but all with the density correction algorithm as a default treatment. The effects of each of these treatments on the pressure and on the free surface profiles are analyzed by comparing our numerical findings with experimental and numerical results in the literature. After the detailed scrutiny on the dam-break problem, sway-sloshing problem is handled with the VXSPH+APD algorithm which has been noted to provide the most reliable and accurate results in the dam-break problem. For the sway-sloshing problem, the time histories of free surface elevations on the left side wall of the rectangular tank are compared with experimental and numerical results available in the literature. It was shown that the VXSPH+APD treatment significantly improves the accuracy of the numerical simulations for violent flows with a free surface and lead to the results which are in very good agreement with experimental and numerical findings of literature in terms of both the kinematic and the dynamic point of view.

1. Introduction

Due to its Lagrangian and meshless nature, the Smoothed Particle Hydrodynamics (SPH) method is an exceptionally suitable tool for modeling highly nonlinear violent flows with a free surface. The SPH method was introduced simultaneously by Gingold and Monaghan [3] and Lucy [4] to simulate compressible flow problems in astrophysics and later extended by Monaghan [1] to model incompressible free surface flows through using a Weakly Compressible SPH approach (WCSPH) which assumes that a fluid is incompressible if its density variation is less than 1%. In the SPH method, the continuum is represented by particles which carry fluid properties such as

density, velocity and pressure, among others. These particles represent infinitesimally small fluid elements having finite volumes, and can interact with each other in each time-step through a weight function having a compact support domain. The relevant governing equations and boundary conditions are discretized in space over these particles. Although the WCSPH method has numerous advantages on solving nonlinear engineering problems with large and rapid deformations in the topology of fluid such as shock [5], high velocity impact [6], underwater explosion [7] and violent free surface hydrodynamics [8] problems, it still requires a detail scrutiny to understand the effect of numerical remedies (i.e., particle distribution regularization through XSPH, density correction, and some others) incorporated into the standard WCSPH method on the accuracy of the solution. As shown in our earlier work [9] as well as in another work by Molteni and Colagrossi [10], the kinematics of violent flows with free surface might be easily captured correctly to a certain extent by using the conventional WCSPH algorithm with commonly

* Corresponding author.

E-mail addresses: ozbulutm@itu.edu.tr (M. Ozbulut), meyildiz@sabanciuniv.edu (M. Yildiz).

used formulations in the SPH literature. However, noting that the WCSPH method is known to produce an oscillatory pressure field due to the fact that the pressure is calculated from density variation through an equation of state [10,11], the existence of large and random oscillations in the pressure field urges SPH practitioners to develop new numerical correction algorithms to have realistic pressure values.

In order to circumvent pressure related problems, there have been some attempts whereby to improve the accuracy, stability and robustness of numerical solution. In addition to Monaghan's [12] "artificial viscosity" and "XSPH velocity variant" terms which have received noticeable acceptance, and in turn have been widely used by SPH researchers, new numerical remedies or corrective algorithms have also been incorporated into SPH method in recent studies. Molteni and Colagrossi [10] added a density diffusion term into the mass conservation equation, which is a pure numerical effect and goes to zero as the number of particles increases. To prevent particle penetration, Zheng and Duan [13] added an extra position corrector term to the positions of the particles. They stated that this additional term has a positive effect on the homogeneous distribution of particles which leads better pressure fields in the problem domain.

Present work compares numerical remedies namely, density correction, XSPH velocity variant algorithm commonly used in the SPH literature among each other and with a relatively recent one referred to as Artificial Particle Displacement (APD) [2]. It also introduces a new treatment for free surface problems, which uses a hybrid combination of velocity updated XSPH, which is hereafter referred to as VXSPH, algorithm for the free surface particles and APD for the rest of fluid particles. Two dimensional dam-break problem, which is quite well-accepted as a benchmark test case among SPH researchers, is solved using Euler's equation of motion. Having validated the numerical results by those given in the literature for the dam-break problem, a two dimensional sway-sloshing problem is modeled to further test the numerical treatment which has been observed to give the most accurate and reliable results in the numerical stimulation of dam-break problem.

The present work initially considers the numerical modeling of the dam-break problem through employing the conventional basic formulations of the WCSPH method together with the artificial viscosity term. It is understood that the standard WCSPH formulations without any numerical remedies lead to significant oscillations in density field and in turn in pressure distributions, thereby resulting in particle deficient region (a gap) in the vicinity of the solid wall at the front edge of the flow. In order to eliminate the noise in pressure field, the density correction treatment is employed as a numerical remedy to the conventional WCSPH method since the pressure value of a particle is calculated by an artificial equation of state [14], which directly relates the density and pressure of particles. The density correction is considered as a baseline treatment while other three numerical treatments (namely, XSPH, APD, and VXSPH) modeled here are used together with the density correction algorithm individually or in a combined manner. The density correction treatment is applied in the predictor step and the new pressures are computed by using the corrected density values.

After confining the pressure oscillations within an admissible range by using the density correction algorithm, the effects of the other three different numerical remedies on the pressure, on the free surface elevation and on the total mechanical energy of the fluid particles are investigated systematically. The first of these treatments is the well-known XSPH algorithm which was suggested by Monaghan [1] for high speed free surface flows to keep the particles orderly and to prevent a particle penetration one by another. The second one is the method implemented in order to eliminate particle clustering and fractures due to the tendency of SPH particles

to follow streamline trajectories, wherefore a more homogeneous particle distribution can be achieved in the computational domain. Presently, the APD method is further extended to a flow problem with a violent free surface since in the literature it was originally used for flow problems with bounding solid boundaries [15]. In the light of the results of the first two remedies, the hybrid combination of APD and VXSPH algorithms is used wherein the VXSPH method is applied only to the particles near the free surface and the APD treatment is applied only to fluid regions away from the free surface and fully populated with particles. In SPH modeling of free surface problems, particles may escape from free surface, which is a numerical artifact and becomes much more noticeable as the velocity and the non-linearity of the flow increases. The VXSPH algorithm provides an artificial surface tension force for free surface particles thereby impeding the escape of individual particles from the free surface and keeping these particles being attached to the free surface. The results of simulations for the dam-break problem show that the combined usage of VXSPH and APD treatments gives the most reliable and admissible results from both kinematical and dynamical point of view. The VXSPH-APD hybrid treatment used in the dam-break problem is further validated for another challenging free surface problem, namely, two dimensional sway-sloshing wherein the free surface elevations on the left side wall are compared with the experimental data and numerical solutions of the studies given by Pakozdi [16] and Molteni [10].

2. Governing equations and numerical modeling

2.1. Field equations

In the free surface hydrodynamics, the effect of viscosity is generally assumed to be negligible and the fluid particles are allowed to have rotational motion which leads the equation of motion governed by Euler's equation:

$$\frac{d\vec{u}}{dt} = -\frac{1}{\rho}\nabla P + \vec{g} \quad (1)$$

$$\vec{u} = \frac{d\vec{r}}{dt} \quad (2)$$

where, \vec{u} , \vec{r} , P and ρ are the velocity, position, pressure and density of particles, respectively, and \vec{g} is the gravitational acceleration. In addition to Euler's equation of motion, the continuity equation employed is as follows:

$$\frac{d\rho}{dt} = -\rho\nabla \cdot \vec{u}. \quad (3)$$

In the SPH method, there are two general approaches for enforcing the incompressibility condition, namely, the weakly compressible SPH (WCSPH), and the incompressible SPH (ISPH) methods, which differ from each other in terms of how the pressure in the equation of motion is computed. The WCSPH method uses an explicit artificial equation of state that couples the density with the pressure through a coefficient widely referred to as the speed of sound. This approach stems from the initial applications of the SPH method to the compressible fluid flow problems on the fact that all fluids may be regarded as weakly compressible, at least theoretically. The equation of state enforce the incompressibility condition on the flow such that a small variation in density produces a relatively large change in pressure thereby limiting the dilatation of the fluid to one percent. The ISPH technique is based on the projection method originally proposed in [17], which is referred to as the standard projection or the divergence-free ISPH method. In this method, the pressure term in the equation of motion is computed by solving a pressure Poisson equation with

the divergence of the intermediate velocity being a source term. There are several recent works which have aimed to compare WCSPH and ISPH methods for free surface and bluff body problems [17,18]. Major advantages of WCSPH over ISPH are the ease of programming, and better ordered particle distributions. Mainly for these reasons, the WCSPH method has become the most widespread approach to solve the linear momentum balance equation in the SPH literature. The standard WCSPH approach requires the usage of a Mach (M) number (a dimensionless quantity representing the ratio of speed of fluid to speed of sound) less than 0.1 to ensure that the flow is incompressible and to avoid the formation of unphysical void regions in the computational domain. The WCSPH approach unlike the ISPH method needs to use extremely small time steps in order to satisfy the Courant–Friedrichs–Lewy (CFL) condition since the speed of sound has a direct effect on the permissible time-step in a given simulation, which directly affects the total simulation time [2,19]. There are various forms of artificial equation of state used within the scope of WCSPH approach to be able to calculate the pressure for computing pressure gradient term in the equation of motion. In this work, the one proposed by Monaghan [12] is used:

$$p = \frac{\rho_0 c_0^2}{\gamma} \left[\left(\frac{\rho}{\rho_0} \right)^\gamma - 1 \right], \quad (4)$$

where c_0 is the reference speed of sound, γ is the specific heat-ratio of water and is equal to 7 and ρ_0 is the reference density which is equal to 1000 [kg/m³] for fresh water. The value of reference speed of sound is determined by M . It is required that $M \sim 0.1$ to keep density variation around 1% [12]. The key point in Eq. (4) is that a very small variation in the density of the fluid particle leads to a relatively large change in pressure whereby the volume change of particles is restricted around 1%. Furthermore, it should be noted that the larger the value of c_0 , the smaller the value of permissible time step, Δt due to the CFL stability condition. Hence, to avoid the unnecessary increase in the computational time, c_0 should be small enough while guaranteeing the incompressibility condition. In the simulations of the dam-break and sway-sloshing problems, c_0 is taken as 50 [m/s] and 40 [m/s], respectively.

2.2. Discretization of governing equations in SPH method

SPH is a Lagrangian method where the flow domain is represented by a finite number of movable particles which can carry the characteristic properties of the problem at hand such as mass, position, velocity, momentum, and energy. The core of its mathematical formulation is based on the interpolation process, wherefore the fluid system is modeled through the interaction among particles, which is achieved by an analytical function widely referred to as the kernel/weighting function $W(r_{ij}, h)$ where r_{ij} is the magnitude of the distance vector, $\vec{r}_{ij} = \vec{r}_i - \vec{r}_j$ for a pair of particles, namely, the particle of interest \mathbf{i} and its neighboring particles \mathbf{j} , and h is the smoothing length. Here, \vec{r}_i and \vec{r}_j are the position vectors for the particle \mathbf{i} and \mathbf{j} , respectively, and as to be understood, boldface indices \mathbf{i} and \mathbf{j} are particle identifiers to denote particles. An arbitrary continuous function (which can be scalar, vectorial, or tensorial), $A(\vec{r}_i)$, or concisely denoted as A_i , can be interpolated as

$$A_i \cong \langle A(\vec{r}_i) \rangle \equiv \int_{\Omega} A(\vec{r}_j) W(r_{ij}, h) d^3 \vec{r}_{ij}, \quad (5)$$

where the angle bracket " $\langle \rangle$ " denotes the kernel approximation, $d^3 \vec{r}_{ij}$ is the infinitesimal volume element inside the domain, and Ω represents the total bounded volume of the domain. The function A_i may represent any hydrodynamic properties such as velocity, pressure, density, and viscosity. The kernel function

used in the current work is a quintic spline with the form of

$$W(R, h) = \alpha_d \begin{cases} (3-R)^5 - 6(2-R)^5 + 15(1-R)^5, & 0 \leq R < 1 \\ (3-R)^5 - 6(2-R)^5, & 1 \leq R < 2 \\ (3-R)^5, & 2 \leq R < 3 \\ 0, & R \geq 3 \end{cases} \quad (6)$$

where $R = r_{ij}/h$ and α_d is a coefficient that depends on the dimension of the problem such that $120/h$, $7/(478\pi h^2)$ and $3/(359\pi h^3)$ for one, two and three dimensions, respectively [20]. Upon using the SPH approximations which involve the replacement of the integral operation over the volume of the bounded domain by the mathematical summation operation over all neighboring particles \mathbf{j} of the particle of interest \mathbf{i} , and the differential volume element by the m_j/ρ_j , and performing some tedious mathematical manipulations, the Euler's equation of motion and the mass conservation can respectively be discretized by the SPH method as

$$\frac{d\vec{u}_i}{dt} = - \sum_{j=1}^N \left(\frac{p_i}{\rho_i^2} + \frac{p_j}{\rho_j^2} + \Pi_{ij} \right) \nabla_i W_{ij} \quad (7)$$

$$\frac{d\rho_i}{dt} = \rho_i \sum_{j=1}^N \frac{m_j}{\rho_j} (\vec{u}_i - \vec{u}_j) \cdot \nabla_i W_{ij}. \quad (8)$$

Here, m_j is the mass of the particle \mathbf{j} , ∇_i is the gradient operator where the particle identifier \mathbf{i} indicates the spatial derivative is evaluated at particle position \mathbf{i} , and Π_{ij} is the artificial viscosity term as

$$\Pi_{ij} = \begin{cases} -\alpha \mu_{ij} \frac{c_i + c_j}{\rho_i + \rho_j}, & \vec{u}_{ij} \cdot \vec{r}_{ij} < 0 \\ 0, & \vec{u}_{ij} \cdot \vec{r}_{ij} \geq 0 \end{cases}, \quad (9)$$

$$\mu_{ij} = h \frac{(\vec{u}_i - \vec{u}_j) \cdot (\vec{r}_i - \vec{r}_j)}{\|\vec{r}_i - \vec{r}_j\|^2 + \theta h^2}. \quad (10)$$

The inclusion of the artificial viscosity term in the Euler equation of motion is necessary to increase the stability of the numerical procedures through adding some diffusion to numerical solution. However, the magnitude of the artificial viscosity coefficient should also be small enough to prevent the occurrence of the viscous effects during the fluid flow. The numerical value of α utilized in this work is determined through comparing the obtained numerical results with benchmark solutions. In the simulation of dam-break and sway-sloshing problems, the parameters α and θ are taken as 0.06 and 0.05, respectively. The local speed of sounds in Eq. (9) is found according to the relation $c_i = c_0(\rho_i/\rho_0)^{(\gamma-1)/2}$.

2.3. Boundary conditions

The accurate force transfer from solid boundary particles onto the fluid particles is modeled through utilizing ghost particle technique whereby fluid particles, having a vertical distance less than 1.55 h from the solid boundary, or in other words, within the support domain of boundary particles, are mirrored with respect to the solid wall to create ghost particles outside the flow domain. Ghost particles are endowed with field variables (i.e., velocity and pressure) in accordance with the boundary conditions to be implemented. For the Dirichlet boundary condition, the following linear interpolation is employed; namely, $\Lambda_g = 2\Lambda_b - \Lambda_f$ while for the Neumann boundary condition, ghost particles are given the same fields values as their corresponding fluid particles, and hence, $\Lambda_g = \Lambda_f$, where Λ_g , Λ_b , and Λ_f are in the given order represent the fields variables associated with the ghost, boundary, and fluid particles. In the simulations of present work for both dam-break and sway-sloshing problems, walls are modeled with

free slip boundary condition. In dam-break problem, for the horizontal wall, the ghost particle velocities are evaluated by $\partial u_x / \partial z = 0$, and $u_z = 0$, necessitating that $u_{x,g} = u_{x,f}$ and $u_{z,g} = -u_{z,f}$ while for the vertical walls, $\partial u_z / \partial x = 0$, and $u_x = 0$, requiring that $u_{z,g} = u_{z,f}$ and $u_{x,g} = -u_{x,f}$ [2]. As for the boundary conditions for the sway-sloshing problem where the walls have a harmonic motion, the free slip boundary condition on the horizontal wall requires $u_{x,g} = 2u_{x,b} - u_{x,f}$ and $u_{z,g} = -u_{z,f}$, and for the vertical walls it requires that $u_{x,g} = 2u_{x,b} - u_{x,f}$ and $u_{z,g} = u_{z,f}$. The pressure boundary condition on the solid walls is enforced as $\nabla p \cdot \vec{n} = 0$, which requires that $\rho_g = \rho_f$ and $p_g = p_f$. As in the case of fluid particles, the density of boundary particles is computed through the solution of the continuity equation given in Eq. (3) and these densities are smoothed by using Eq. (12). Upon determining the density of boundary particles calculated, pressure of boundary particles is computed by the usage of previously introduced equation of state. Due to the dynamic nature of the problems solved in this work, some boundary particles may not have enough neighboring fluid particles for accurate calculation of density of boundary particles. In such a case, these boundary particles should not feel any pressure force from surrounding fluid particles. Owing to the density correction through smoothing, boundary particles with no or insufficient neighboring fluid particles will acquire density and in turn pressure because of the transfer of data among boundary particles. To avoid this, and be able to calculate the pressure of boundary particles correctly, the density of boundary particles with less than ten fluid particles is set back to reference density, which corresponds to enforcing zero pressure for these boundary particles. The free surface boundary condition is enforced by setting the pressure of particles close to free surface to the atmospheric pressure through taking the densities of these particles as reference density. The decision whether a particle should be regarded as a free surface particle depends on the number of neighbor particles of the given particle. In the simulations presented, the average number of neighbor particles is around 40–45 at each time step. Thus, a fluid particle with less than twenty-five neighbors is considered as a free surface particle.

2.4. Time integration

The time integration scheme used in this work is a predictor–corrector one wherein particle positions, densities and velocities are updated in the following manner, respectively:

$$\frac{d\vec{r}_i}{dt} = \vec{u}_i, \quad \frac{d\rho_i}{dt} = k_i, \quad \frac{d\vec{u}_i}{dt} = \vec{a}_i. \quad (11)$$

The time integration starts with the prediction of the intermediate positions and densities of the particles by $\vec{r}_i^{(n+1/2)} = \vec{r}_i^{(n)} + 0.5\vec{u}_i^n \Delta t$ and $\rho_i^{(n+1/2)} = \rho_i^n + 0.5k_i^n \Delta t$. The pressure values are calculated from Eq. (4) by using the intermediate densities while new time steps' velocities are computed by $\vec{u}_i^{(n+1)} = \vec{u}_i^{(n)} + \vec{a}_i^{(n+1/2)} \Delta t$. Finally, at the corrector step, the particle positions and densities are updated at half time step as $\vec{r}_i^{(n+1)} = \vec{r}_i^{(n+1/2)} + 0.5\vec{u}_i^{(n+1)} \Delta t$ and $\rho_i^{(n+1)} = \rho_i^{(n+1/2)} + 0.5k_i^{(n+1)} \Delta t$. The superscript n is a temporal index.

3. Numerical treatments

The main focus of this paper is on the comparison of the effects of different numerical remedies on the accuracy and robustness of the WCSPH method. These remedies include density (Shephard)

correction, XSPH velocity correction, and artificial particle displacement (APD), which have been widely utilized in the SPH literature to circumvent the short comings of standard SPH formulations such as pressure oscillation, non-uniform and clustered particle distributions, among others. To be able to quantify the effects of these treatments on the numerical results and also be able to investigate their hybrid usage, two important benchmark problems, namely dam-break and sway-sloshing, are modeled. The dam-break problem is solved using all these remedies and results are compared to each other in terms of free surface profiles and pressure contours before fluid particles hit to the right wall. Moreover, for each remedy, the pressure values time series at a point on the right vertical wall are compared with the experimental data given in the literature [10,16] after the fluid particles hit to the right wall. For the sake of completeness, in following we concisely elaborate on each individual numerical remedy which are listed previously.

Density correction algorithm: In the WCSPH approach, the precise calculation of density field is very critical since the pressure is directly coupled to density through the artificial equation of state. Without the density correction treatment, the pressure fields in the problem domain can oscillate excessively and become unstable due to the numerical noise generated in the standard SPH formulations. The inclusion of the density correction algorithm into the numerical scheme notably improves pressure distributions, especially close to the solid boundaries. In this work, the density correction is used as a baseline treatment and always employed with other numerical remedies through the formulation

$$\hat{\rho}_i = \rho_i - \sigma \frac{\sum_{j=1}^N (\rho_i - \rho_j) W_{ij}}{\sum_{j=1}^N W_{ij}} \quad (12)$$

where $\hat{\rho}$ is the corrected density, N is the number of neighbor particles for particle i and σ is a constant which is set to unity in this work thereby leading to well-known ‘‘Shephard’’ interpolation in the SPH literature [21].

XSPH velocity variant algorithm: It is to be noted that in the SPH method, the order of particles affects the accuracy of interpolations for the computations of gradient and Laplacian of fields. Therefore, for computational stability and accuracy, it is highly desirable to move the particles in a more orderly fashion. To achieve this, Monaghan [1] proposed and utilized the XSPH velocity variant algorithm for free surface flows which later has become one of the widely used and well-known numerical remedies for improving the particle distribution. In the XSPH method, the velocity computed through the solution of equation of motion is modified such that it includes the contribution from neighboring particles, thereby coaxing fluid particles to move with a velocity (similar to the average velocity), $\vec{u}_i^{xsph} = \vec{u}_i - \Delta \vec{u}_i$ through advection equation $d\vec{r}_i/dt = \vec{u}_i^{xsph}$ where $\Delta \vec{u}_i$ is the velocity variant defined as

$$\Delta \vec{u}_i = \varepsilon \sum_{j=1}^N \frac{m_j}{\bar{\rho}_{ij}} (\vec{u}_i - \vec{u}_j) W_{ij}. \quad (13)$$

Here, $\bar{\rho}_{ij} = (\rho_i + \rho_j)/2$ and ε is a constant commonly taken as 0.5 in the SPH literature [16]. To avoid the error due to the density fluctuations in the velocity variant, it is prudent to modify Eq. (13) as

$$\Delta \vec{u}_i = \varepsilon \frac{\sum_{j=1}^N (\vec{u}_i - \vec{u}_j) W_{ij}}{\sum_{j=1}^N W_{ij}} \quad (14)$$

Artificial particle displacement (APD) algorithm: Being a numerical tool based on interpolation theory, the SPH method requires that particles be distributed as uniformly as possible for the robustness and the accuracy of numerical models. If particles in the problem

domain acquire a non-uniform and clustered distribution as a result of solution, it is no longer possible to retain the stability and the reliability of numerical results, and in extreme cases, the numerical algorithm may break down. Shadloo et al. [2] in flow simulations with bounded domains added a small artificial particle displacement term to the position vectors of each particle to disturb the particle trajectory thereby impeding particle clustering and showed that the APD method is extremely effective in preserving particle uniformity, and in turn improving the both the robustness and the accuracy of the SPH computation. The APD term $\delta \vec{r}_i$ is given as

$$\delta \vec{r}_i = \beta \sum_{j=1}^N \frac{\vec{r}_{ij}}{r_{ij}^3} r_o^2 v_{\max} \Delta t \quad (15)$$

where β is a parameter which is equal to 0.05 in this work, $r_o = \sum_j r_{ij}/N$ is the cut-off distance and v_{\max} is the maximum velocity in the problem domain in every time step. The parameter β should be small enough not to change the physics of the flow and large enough for providing a homogeneous and uniform particle distribution. In this work, the numerical value of the coefficient β is chosen relying on the simulation results of many different benchmarks problems solved in our previous works [2,15]. Additionally, it is noted that the value of APD added to the numerical simulations is less than 0.1% of the physical particle displacement for a given time step. Hence, one may directly conclude that the APD does not alter the neighbors of the given particle of interest, and thus do not introduce errors to the solution that changes the physics of the problem at hand. The APD algorithm is employed only for fully populated flow regions.

Combined XSPH and APD algorithm: The treatment of free surface is always a challenge in the modeling of hydrodynamics and generally requires a special care to obtain accurate surface profile. A combined usage of XSPH and APD treatments is also investigated as a final numerical remedy where a slightly different implementation of standard XSPH algorithm is used only for the particles on the free surface while the APD algorithm is employed for the fully populated flow regions. The physical regions in the computational domain where the algorithms are applied are illustrated in Fig. 1.

Recall that in the standard XSPH algorithm, the velocity variant is appended to the velocity when advancing the particle position only, but does not affect the velocity used for other SPH calculations. On the other hand, in the hybrid treatment presented here, the XSPH velocity \vec{u}_i^{xsph} is utilized for both advancing the position of particles and replacing the fluid velocity, namely, $\vec{u}_i = \vec{u}_i^{xsph}$, which means that the fluid velocity computed through the solution of the equation of motion is substituted by the average velocity. This modified velocity is then used for all other SPH calculations such as the solution of mass and momentum balance equations for density and velocity. This new treatment is hereafter referred to as velocity updated XSPH algorithm with the abbreviation of VXSPH. Since the VXSPH is applied only to a very thin free

surface layer (like first two rows of free surface particles), it does not change the physical behavior of the flow. The VXSPH acts like a surface tension force thus keeping particles orderly on the free surface. The ε parameter for VXSPH treatment is chosen to be relatively smaller than the one for XSPH with the numerical values of 0.0025 in the dam-break and 0.005 in the sway-sloshing simulations. The APD treatment on the other hand disturb the trajectories that particles follow whereby to result in more homogeneous particle distribution in the fully populated areas.

4. Numerical results

The numerical treatments explained in the previous section are applied to the two dimensional dam-break problem sequentially and the effect of each treatment on the results is presented comparatively. Subsequently, the numerical treatment that gives physically the most reasonable and accurate results in the dam-break problem is used for the two dimensional sway-sloshing problem and numerically computed free surface elevations on the walls of the tank are compared with the experimental results given in [16].

4.1. Dam-break problem: the comparison of the numerical treatments

The dam-break problem wherein initially stagnant water reserve starts suddenly to move toward the other wall is a commonly used benchmark problem for the free surface simulations in the SPH literature [13,22,23]. The modeling domain and geometry of the 2-D dam-break problem is given in Fig. 2 where the length parameters H_w , L_w and L are equal to 0.6 [m], 1.2 [m] and 3.23 [m], respectively and the initial pressure field of the water reserve is set to the hydrostatic pressure. All particles have the same initial particle spacing (dx) which is equal to 0.01 [m] and the smoothing length is taken as $1.33dx$. 7381 fluid particles and 525 solid boundary particles are used during the simulations. In addition to solid boundary particles, ghost particles are generated in every time step and hence, the total number of particles becomes nearly 9000. The time step value is determined from the CFL condition where the recommended time step is $\Delta t \leq C_{CFL} h_{ij,\min}/(C_i + v_{\max})$ [24]. Here $h_{ij} = 0.5(h_i + h_j)$ and $h_{ij,\min}$ is the minimum smoothing length among all i - j pairs which is a constant in this work. C_{CFL} number should be $0 \leq C_{CFL} \leq 1$. In this work, C_{CFL} value is chosen to be 0.4 for dam-break and 0.5 for sway-sloshing problems. To address the shortcomings of standard SPH equations and to make a clear list of remedies that need to be implemented, the present study has initially simulated the dam-break problem by using the standard SPH equations without any numerical remedies. In the light of these simulation results, it is noted that the standard SPH treatment results in inaccurate pressure fields throughout the simulation,

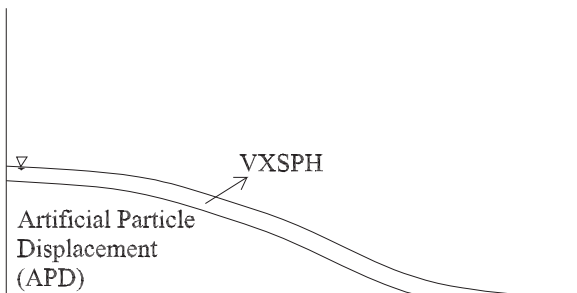


Fig. 1. The sketch of the physical regions that VXSPH and APD algorithms are active.

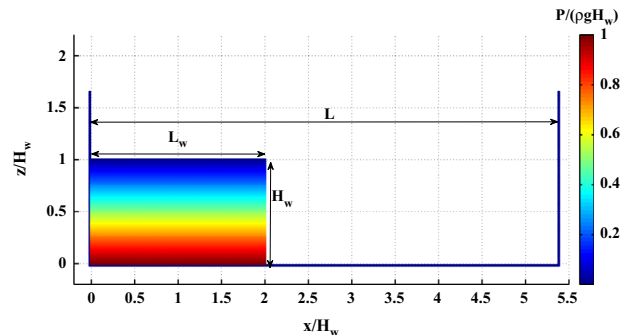


Fig. 2. The model domain and geometry for dam-break problem.

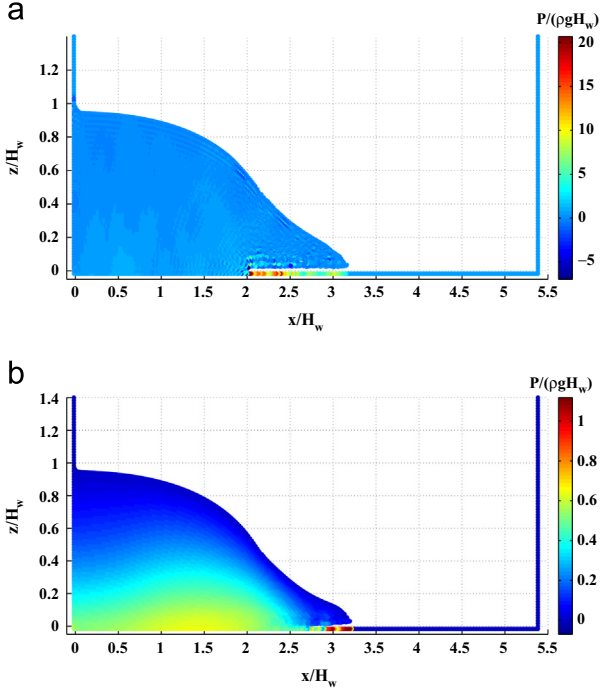


Fig. 3. Comparing pressure $P/(\rho g H_w)$ contours at $t = 1.21(H_w/g)^{0.5}$. (a) Pressure $P/(\rho g H_w)$ contours without density correction and (b) pressure $P/(\rho g H_w)$ contours with density correction.

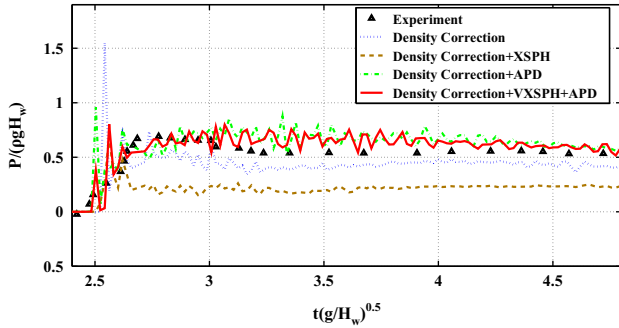


Fig. 4. Time histories of Pressure $P/(\rho g H_w)$ values after the hit of water to the right wall.

which becomes particularly significant at the front edge of the flow thereby causing unphysical fracture or gap between the wall and the fluid particles, (see Fig. 3(a) for the pressure distribution and the gap at $t = 1.21(H_w/g)^{0.5}$). It is observed that the problem in pressure and consequent gap is directly related to the calculation of density through using Eq. (8) without any density correction algorithm. In this direction, as a first remedial treatment, the density correction term given in Eq. (12) is added to the algorithm and the pressure distribution of the new simulation at the same instant is provided in Fig. 3 as a comparison. One can note the obvious improvement in computed pressure values and that there is no longer a gap between solid boundary and leading edge of flow as a direct result of the density correction treatment. After incorporating the density correction to standard SPH algorithm for improving the accuracy of the computed pressure field, XSPH, then APD and finally combined VXSPH and APD treatments are appended to the SPH algorithm sequentially. In Fig. 4, the pressure time series after the impact of the water reserve to the right wall of the tank are compared with the experimental data given by [10]. The pressure values are calculated on the right wall at $z = 0.115$ [m] performing interpolation with the quintic kernel function, which corresponds

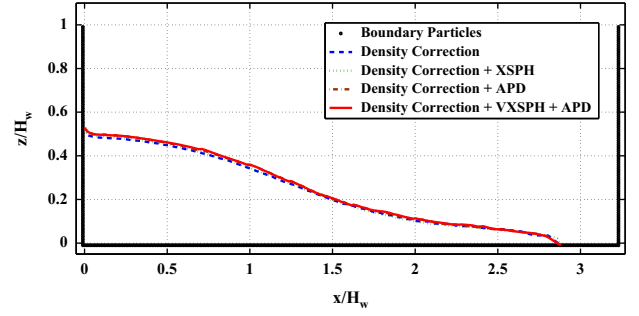


Fig. 5. Free surface profiles at $t = 2.23(H_w/g)^{0.5}$.

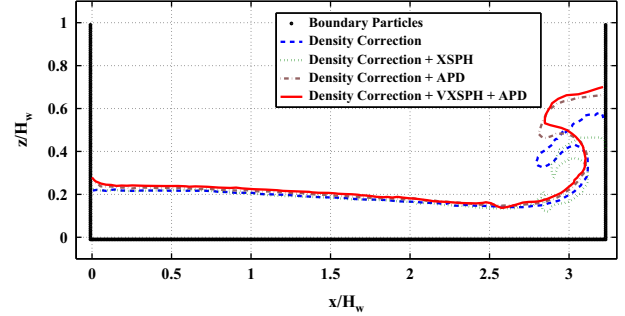


Fig. 6. Free surface profiles at $t = 5.34(H_w/g)^{0.5}$.

to the lower rim of the pressure sensor used in the experimental work of Pakozdi [16]. The oscillation in pressure as seen in Fig. 4 can be attributed to the WSPH approach. To further reduce the oscillations in the pressure field, during the calculation of time series of the pressure values on the right wall ($z = 0.115$ [m]), the smoothing length parameter is chosen to be four times larger than that used in the simulations thereby reducing the oscillations in pressure since the pressure values at the point of interest are calculated by considering larger region. The h value used in acquiring wall pressure is found to be optimum since increasing its value does not change the calculated wall pressure. As can be seen from Fig. 4, the hybrid VXSPH+APD treatment provides the most comparable results with experimental data. It enables accurate prediction of the time at which the flow impacts upon the wall. Furthermore, the pressure values after the impact of the flow are in very good agreement with the experimental data. On the other hand, the density correction treatment predicts the hit of the fluid to the wall with some delay and under estimates the experimentally measured pressure. Similar to results of the simulation with density correction alone, the XSPH velocity variant treatment also captures the instant of the impact of the fluid with small latency, but immediately after the hit of fluid to the right wall, there is a significant drop in pressure values. Having observed the difference in pressure evolutions for different remedies at the right wall, it becomes a necessity to compare the free surface profiles of treatments among each other before and after the water reserve hits the wall. Figs. 5 and 6 show the free surface profiles at $t = 2.23(H_w/g)^{0.5}$ and $t = 5.34(H_w/g)^{0.5}$, respectively, where for plotting convenience, the splashing particles are neglected when the free surface contour is created. Fig. 5 clearly denotes that the free surface profiles of all treatments are nearly the same before the water reserve reaches the right vertical wall. However, one can clearly see from Fig. 6 that the variations in pressure values for each treatment reported in Fig. 4 have profound effect on the free surface profile after the water reserve hit the wall. Another comparative graph for four treatments is given in Fig. 7, which shows the pressure distribution and particle positions on the whole domain at a given instant. It is notable that the VXSPH acts like a surface

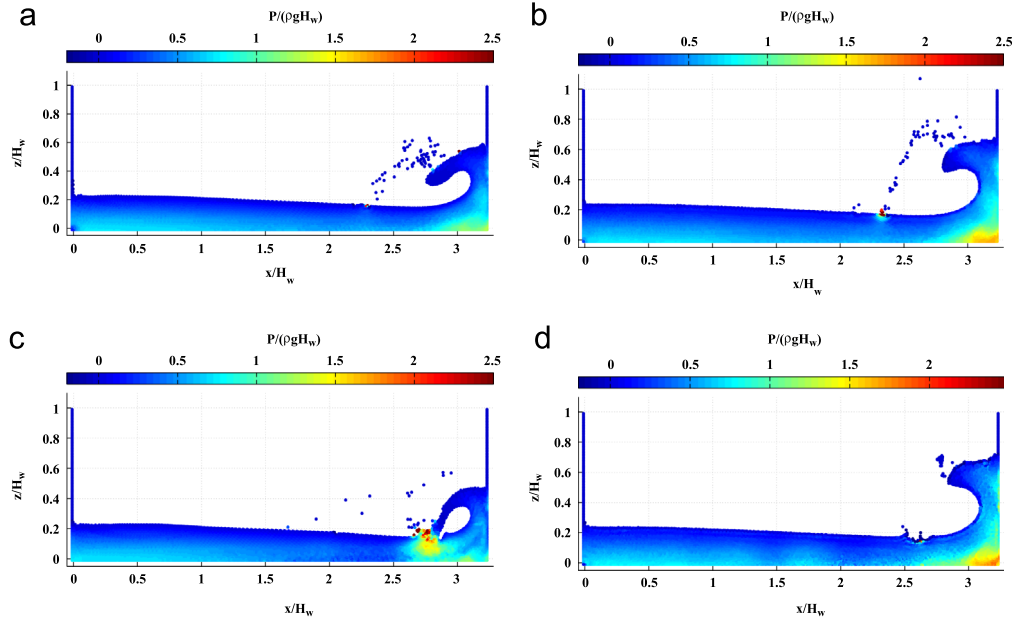


Fig. 7. Comparing the particle positions and pressure fields at $t = 5.34(H_w/g)^{0.5}$. (a) Density correction treatment alone, (b) density correction with APD treatment, (c) density correction with XSPH treatment and (d) density correction with combined VXSPH and APD treatment.

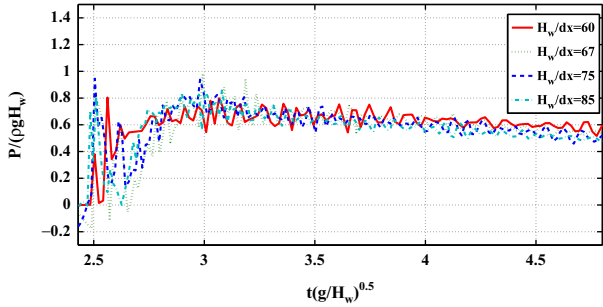


Fig. 8. Convergence study on the pressure values.

tension force for a very thin layer of free surface particles and in turn eliminates the scattering of these particles to large extent especially on the front edge. The pressure values of APD and VXSPH+APD treatments are in mesh with each other as can be seen from Fig. 7(b) and (d) and also from the pressure time series given in Fig. 4, implying that the VXSPH treatment does not alter the physics of the problem. Due to its improvements on the numerical results, the VXSPH+APD treatment is used as a default approach in the simulations performed as a sequel to the dam-break problem. To show the convergence of the numerical solutions, the total number of particles is increased step by step. The total number of fluid particles is determined by using four different H_w/dx ratios which are 60, 67, 75 and 85. These ratios correspond to 7381, 8978, 11,250 and 14,792 fluid particles, respectively. In Fig. 8 variations of dimensionless pressure on the right wall as a function of dimensionless time for four different particle resolutions are given. The comparison of results on these four particle resolutions clearly indicates that the coarse particle number can produce numerical results with satisfactory accuracy given the trade-off between computational costs and capturing flow characteristics of interest. Because finer particle resolutions are computationally expensive, the coarse particle number is chosen for the numerical simulations presented in this paper. As a final data analysis for this test problem, the time evolution of the total mechanical energy is compared for four numerical treatments with the intention of quantifying numerical dissipation incurred. Total

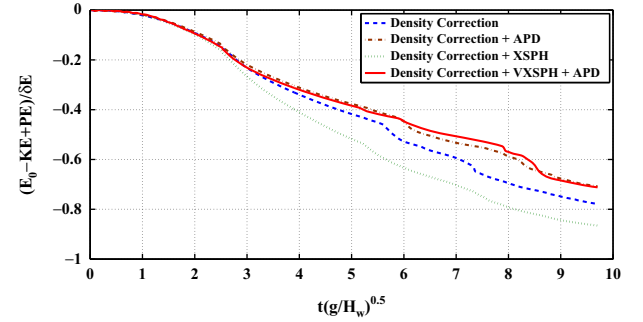


Fig. 9. Time history of the dissipation in mechanical energy.

mechanical energy is computed through summing the total kinetic (KE) and potential (PE) energies of the particles. Fig. 9 shows the variation of dimensionless total mechanical energy, $(E_0 - (KE + PE))/\delta E$ as a function of a dimensionless time where $\delta E = E_f - E_0$, and E_0 and E_f are respectively potential energies at $t=0$ and $t=\infty$, at which the fluid is fully static. The comparison of dissipation rates of the total mechanical energy among the numerical treatments used in the present work shows that the VXSPH+APD treatment conserves the total mechanical energy better than other three treatments since it leads to less numerical energy dissipation.

4.2. Sway-sloshing problem

To further test capability of the VXSPH+APD hybrid treatment, sway-sloshing motion of a partially filled rectangular tank shown is modeled, and numerical results are compared with those of Pakozdi [16]. For the sake of comparison, the geometry of the computational domain as well as the relevant modeling parameters (i.e., amplitude and the angular frequency of the sway motion) is chosen to be the same as those of the reference [16]. The length L and the height H of the tank and the depth of water H_w are respectively 1.73 [m], 1.05 [m], and 0.5 [m]. The input parameters for the current model are: density $\rho = 1000$ [kg/m³], gravitational acceleration $g = 9.81$ [m/s²], initial particle spacing $\Delta x = 0.01$ [m], smoothing length $h = 1.33\Delta x$ [m], artificial viscosity coefficient $\alpha = 0.06$. The total number of particles

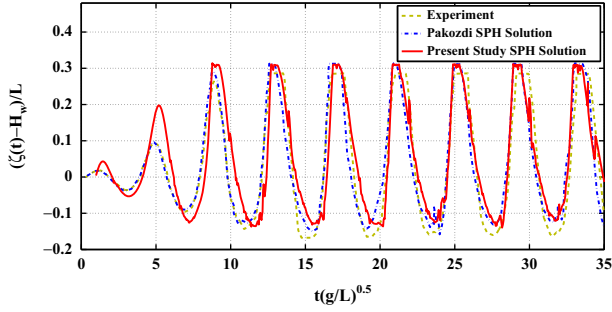


Fig. 10. Comparison of digital time series of the water level evolution close to the left wall where $\xi(t)$ denotes the water level change in time.

in the problem domain is approximately 9500. The initial positions, velocities and pressures of the current test case are set in the same manner as the dam-break problem and the time step used is equal to 0.00015 [s]. Unlike the reference [16] where the sway motion of the tank is modeled by the cosine function for both numerical modeling and experimental study, in this work for numerical convenience, it is prescribed by a sinusoidal function as $x(t) = A \sin(\omega t)$ where A is the amplitude and ω is the angular frequency of the motion. The amplitude and the angular frequency of the sway motion are given as 0.08 [m] and 3.696 [rad/s], respectively, which lead to the period of 1.7 [s] for the harmonic motion of the tank. This preference to use sine function is for avoiding an initial large acceleration and allowing fluid particles to start their motion smoothly. Figs. 10 and 11 present the results of the current work as compared to experimental and numerical results in terms of digital time series of free surface elevations for two different positions of the tank, (namely, close to the left wall where $x=0.05$ [m] and at the mid section of the tank where $x=0.865$ [m]). It can be seen from Fig. 10 that the periods and the amplitudes of the harmonic motion of the fluid are in very good agreement with the numerical results and experimental data of the literature. Wave elevations recorded and computed at the middle of the tank are presented in separate plots in Fig. 11 (to avoid confusion due to crabby nature of the curves). As the data frequency at the middle of the tank is twice the frequency close to the wall, showing all the results on the same figure results in the scratchy and crabbled data presentation. Therefore, we have presented them in separate subplots given in Fig. 11 plots. As a final output of this study, the free surface profiles and the pressure distributions at given instants are shown in Fig. 12. It is from the figures that the VXSPH+APD treatment provides satisfactory particle distribution and free surface profiles wherein particle clustering and particle splashing or separation from the free surface are eliminated.

5. Concluding remarks

In this work, two important 2-D nonlinear violent free surface problems, namely dam-break and sway-sloshing are numerically simulated by utilizing the SPH method. On the one hand, the main objective of this study is to show the proven capability of the SPH method for modeling violent free surface flows, while on the other hand to underline that the SPH technique may still require some special treatments or fine-tuning to improve the accuracy of the solutions. Towards this end, a 2-D dam-break problem is modeled as a benchmark test case with several special remedies elaborated in the body of this work through solving continuity and Euler's equations by the WCSPH approach. The artificial viscosity term is added to the Euler's equation to preserve the stability of the numerical solution. The effects of these special numerical treatments, namely, density correction, the XSPH velocity variant, APD, and an hybrid combination of velocity updated XSPH (VXSPH) and

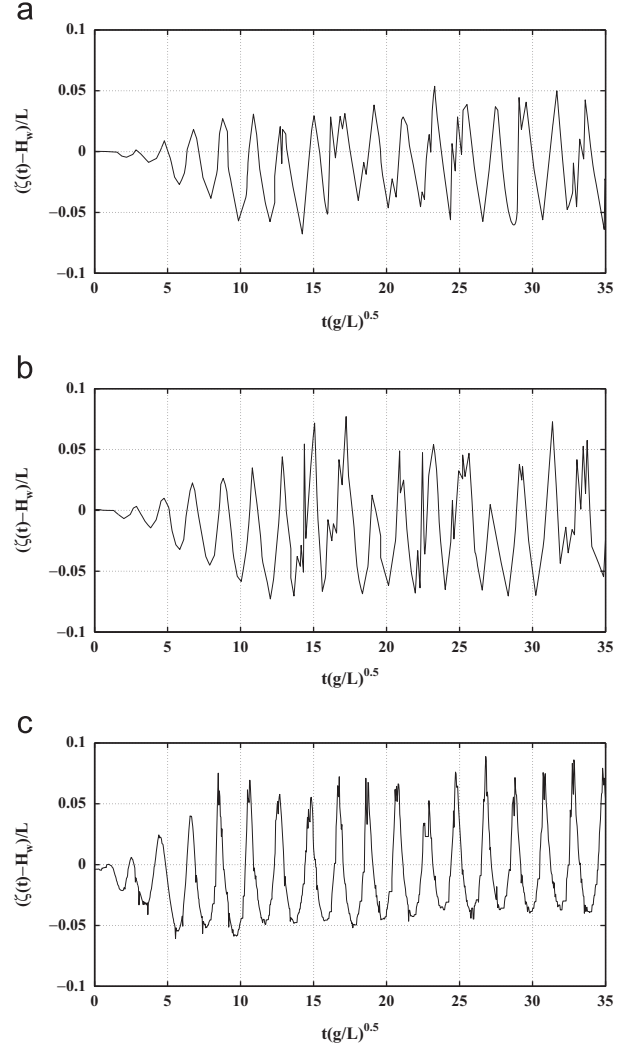


Fig. 11. Comparing the free surface elevations at $x=0.865$ [m]. (a) Experimental results reported in [16]. (b) SPH results reported in [16] and (c) the results of the current study.

APD treatments are compared quantitatively. Initially, the conventional SPH equations are utilized to model the benchmark test case and the examination of the results has suggested that a density correction algorithm is vital for obtaining accurate pressure distributions in computational domain. Subsequently, XSPH velocity variant and APD treatments are also added to the WCSPH algorithm with density correction. It is observed that APD algorithm gives quite compatible results with experimental pressure data on the right wall because of providing a much more homogeneous particle distribution. However, the excessive splashing of particles after the water reserve hit to the right wall disturbs the free surface and hence needs to be circumvented. The free surface profile of the benchmark test cases is improved utilizing a novel approach which is based on the hybrid usage of the VXSPH applied to the free surface particles and APD algorithm applied to the rest of fluid particles. The VXSPH algorithm implemented on the free surface particles alone essentially acts like an artificial surface tension hence keeping free surface particles together. As a second test case, 2-D sway-sloshing problem is handled by only the proposed hybrid numerical treatment which provides the most reliable and accurate results in the dam-break problem. The time histories of the water level elevation at the right wall of the tank are compared with the given experimental and numerical results in Pakozdi's work [16]. Additionally, at given instants, the free surface profiles and the

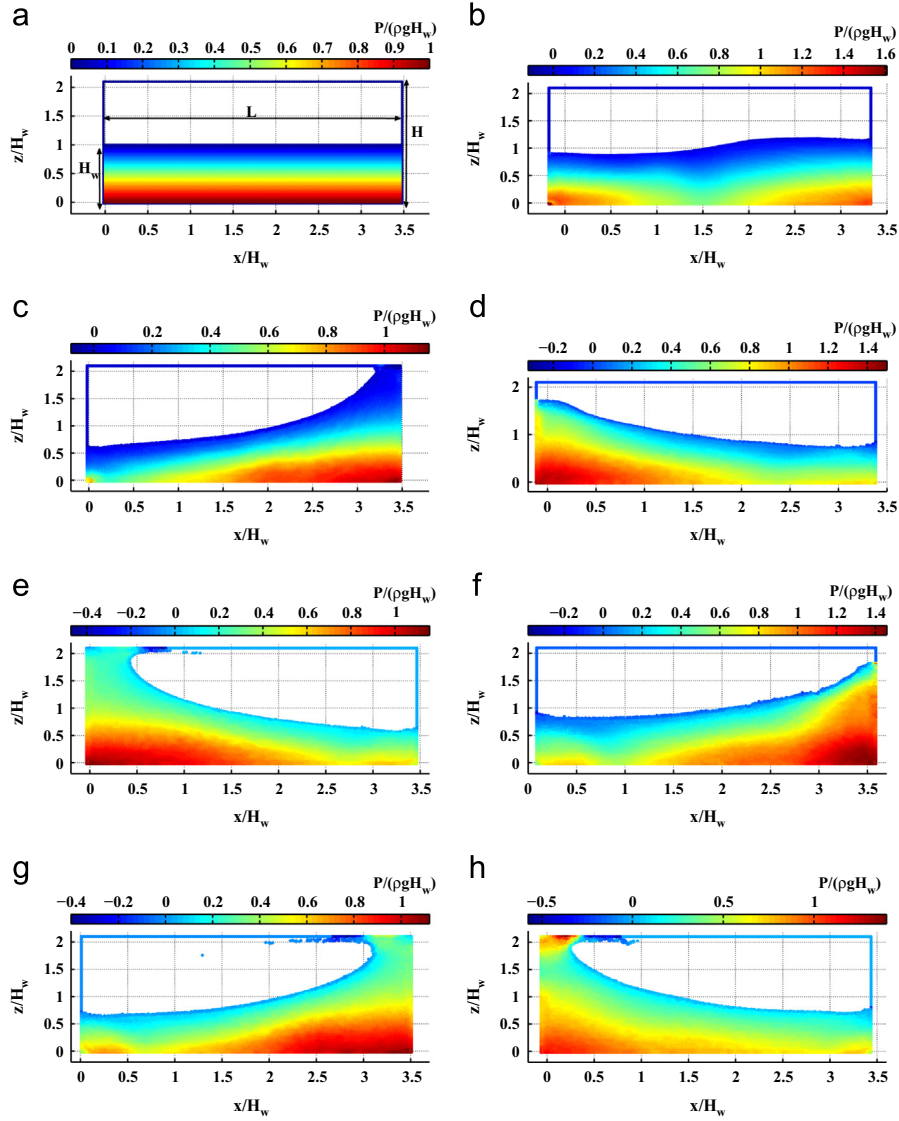


Fig. 12. Particle positions and pressure distributions at given instants. (a) Particle positions and pressure field at $t=0$, (b) particle positions and pressure field at $t=0.38(\text{g/L})^{0.5}$, (c) particle positions and pressure field at $t=2.14(\text{g/L})^{0.5}$, (d) particle positions and pressure field at $t=2.71(\text{g/L})^{0.5}$, (e) particle positions and pressure field at $t=2.83(\text{g/L})^{0.5}$, (f) Particle positions and pressure field at $t=3.40(\text{g/L})^{0.5}$, (g) particle positions and pressure field at $t=3.53(\text{g/L})^{0.5}$ and (h) particle positions and pressure field at $t=4.05(\text{g/L})^{0.5}$.

pressure fields attained in this work are represented sequentially. In light of the obtained results, one may conclude that the hybrid treatment proposed and employed in this work leads to numerical results which are in very good agreement with the experimental and numerical findings of the literature.

Acknowledgments

This work is supported by Ministry of Science, Industry and Technology of Turkey under SAN-TEZ programme with Grant No. 100697-STZ-2010-2.

References

- [1] Monaghan J. Simulating free surface flow with SPH. *J Comput Phys* 1994;110:399–406.
- [2] Shadloo M, Zainali A, Yildiz M, Suleman A. A robust weakly compressible SPH method and its comparison with an incompressible SPH. *Int J Numer Methods Eng* 2011;89(8):939–56.

- [3] Monaghan J, Gingold R. Smoothed particle hydrodynamics: theory and application to non-spherical stars. *Mon Not R Astron Soc* 1977;181:375–89.
- [4] Lucy L. Numerical approach to testing the fission hypothesis. *Astron J* 1977;82:1013–24.
- [5] Liu G, Liu M. *Mesh-free methods: moving beyond the finite element method*. New York: CRC Press; 2003; 379–81.
- [6] Libersky L, Randles P, Carney T, Dickson D. Recent improvement in SPH modeling of hypervelocity impact. *Int J Impact Eng* 1997;20:525–32.
- [7] Swegle J, Attaway S. On the feasibility of using SPH, for underwater explosion calculations. *Comput Mech* 1995;17:151–68.
- [8] Becker M, Teschner M. Weakly compressible SPH method for free surface flow. In: *ACM siggraph symposium on computer animation*. 2007. p. 209–17.
- [9] Ozbulut M, Goren O. Investigation of 2d nonlinear free surface flows by SPH method. In: *Proceedings of the international maritime association of the Mediterranean (IMAM) conference*. Genoa, Italy; 2011. p. 95–100.
- [10] Molteni D, Colagrossi A. A simple procedure to improve the pressure evaluation in hydrodynamic context using the SPH. *Comput Phys Commun* 2009;180:861–72.
- [11] Antuono M, Colagrossi A, Marrone S, Molteni D. Free surface flows solved by means of SPH schemes with numerical diffusive term. *Comput Phys Commun* 2010;181:532–49.
- [12] Monaghan J, Kos A. Solitary waves on a Cretan beach. *J Waterw Port Coast Ocean Eng-Asce* 1999;125(3):145–54.
- [13] Zheng X, Duan W. Numerical simulation of dam-breaking using smoothed particle hydrodynamics and viscosity behavior. *J Mar Sci Appl* 2010;9:34–41.

- [14] Monaghan J. Smoothed particle hydrodynamics. *Rep Prog Phys* 2005;68:1703–59.
- [15] Shadloo M, Zainali A, Sadek H, Yildiz M. Improved incompressible smoothed particle hydrodynamics method for simulating flow around bluff bodies. *Comput Methods Appl Mech Eng* 2011;200:1008–20.
- [16] Pakozdi C. A smoothed particle hydrodynamics study of two-dimensional nonlinear sloshing in rectangular tanks [Ph.D. thesis]. Norwegian University of Science and Technology; 2008.
- [17] Cummins S, Rudman M. An SPH projection method. *J Comput Phys* 1999;152:584–607.
- [18] Lee ES, Moulinec C, Xu R, Violeau D, Laurence D, Stancby P. Comparison of weakly compressible and truly incompressible algorithms for the SPH mesh-free particle method. *J Comput Phys* 2008;227:8417–36.
- [19] Yildiz M, Rook R, Suleman A. SPH with the multiple boundary tangent method. *Int J Numer Methods Eng* 2009;77:1416–38.
- [20] Liu M, Liu G. Smoothed particle hydrodynamics: an overview and recent developments. *Arch Comput Methods Eng* 2010;17:25–76.
- [21] Colagrossi A, Landrini M. Numerical simulation of interfacial flows by smoothed particle hydrodynamics. *J Comput Phys* 2003;191:448–75.
- [22] Marrone S, Antuono M, Colagrossi A, Colicchio G, Le Touze D, Graziani G. δ -SPH model for simulating violent impact flows. *Comput Methods Appl Mech Eng* 2011;200:1526–42.
- [23] Dalrymple RA, Rogers BD. Numerical modeling of water waves with the SPH method. *Coast Eng* 2006;53:141–7.
- [24] Rodriguez P, Bonet J. A corrected smoothed particle hydrodynamics formulation of the shallow water equations. *Comput Struct* 2005;83:1396–410.